Experimental Parasitology 170 (2016) 100–108

Contents lists available at ScienceDirect

Experimental Parasitology

journal homepage: www.elsevier.com/locate/yexpr

Full length article

Hepatic injury associated with *Trypanosoma cruzi* infection is attenuated by treatment with 15-deoxy-$\Delta^{12,14}$ prostaglandin J_2

Federico Nicolás Penas [1], Ágata Carolina Cevey [1], Sofía Siffo, Gerardo Ariel Mirkin, Nora Beatriz Goren*

Instituto de Investigaciones en Microbiología y Parasitología Médica, Facultad de Medicina, Universidad de Buenos Aires, Consejo Nacional de Investigaciones Científicas y Técnicas, Buenos Aires, Argentina

HIGHLIGHTS

- 15dPGJ2 reduces inflammatory cell infiltration in the liver.
- 15dPGJ2 restores the GOT/GPT ratio to normal.
- 15dPGJ2 inhibits the expression of pro-inflammatory mediators in the liver.
- 15dPGJ2 reduces the expression of pro-fibrotic cytokines in the liver.

GRAPHICAL ABSTRACT

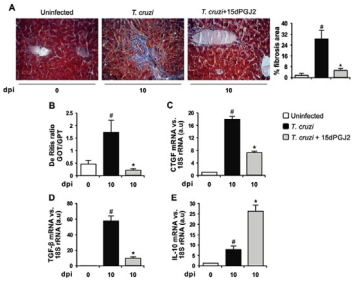

ARTICLE INFO

Article history:
Received 15 July 2016
Received in revised form
14 September 2016
Accepted 27 September 2016
Available online 28 September 2016

Keywords:
Liver
Trypanosoma cruzi
Inflammation
PPARγ
15-Deoxi-Δ^{12-14} prostaglandine J2

ABSTRACT

Trypanosoma cruzi, the etiological agent of Chagas' disease, causes an intense inflammatory response in several tissues, including the liver. Since this organ is central to metabolism, its infection may be reflected in the outcome of the disease. 15-deoxy-$\Delta^{12,14}$ prostaglandin J_2 (15dPGJ2), a natural agonist of peroxisome-proliferator activated receptor (PPAR) γ, has been shown to exert anti-inflammatory effects in the heart upon *T. cruzi* infection. However, its role in the restoration of liver function and reduction of liver inflammation has not been studied yet.

BALB/c mice were infected with *T. cruzi*. The effects of *in vivo* treatment with 15dPGJ2 on liver inflammation and fibrosis, as well as on the GOT/GPT ratio were studied and the role of NF-κB pathway on 15dPGJ2-mediated effects was analysed.

15dPGJ2 reduced liver inflammatory infiltrates, proinflammatory enzymes and cytokines expression, restored the De Ritis ratio values to normal, reduced the deposits of interstitial and perisinusoidal collagen, reduced the expression of the pro-fibrotic cytokines and inhibited the translocation of the p65 NF-κB subunit to the nucleus.

Thus, we showed that 15dPGJ2 is able to significantly reduce the inflammatory response and fibrosis and reduced enzyme markers of liver damage in mice infected with *T. cruzi*.

1. Introduction

Chagas' disease, caused by the protozoan *Trypanosoma cruzi* (*T. cruzi*), affects 6–7 million people worldwide, with an annual incidence of 28 thousand cases in the Americas (WHO, 2016). In

* Corresponding author.
E-mail address: ngoren@fmed.uba.ar (N.B. Goren).
[1] These authors contributed equally to this work.

http://dx.doi.org/10.1016/j.exppara.2016.09.015
0014-4894/

Latin America, this disease is widely distributed, thus causing a serious public health problem. The infection with *T. cruzi* can lead to severe complications in the heart or gastrointestinal tissue, depending on the parasite strain, the host genetics and the route of infection. In addition, it has been recently reported that when there are other underlying diseases, *T. cruzi* infection must be considered as an additional risk factor because it exacerbates liver inflammation and accelerates the development of hepatic injury (Onofrio et al., 2015).

In the past decade, special attention was given to the close relationship between *T. cruzi* infection and liver function. Several research groups have uncovered the interaction between *T. cruzi* and the liver in relation with the role of this organ in the clearance and destruction of blood trypomastigotes (Sardinha et al., 2010). Other studies have focused on the players in the host lipid metabolism (Miao and Ndao, 2014), the damage signals involved in liver immune response during acute infection (Carrera-Silva et al., 2010), or in the liver condition and its functionality in relation to alternative routes of entry of the parasite (Barreto-de-Albuquerque et al., 2015). This interest in the interaction between *T. cruzi* and the liver is based on the fact that the liver is a key organ that controls the metabolic homeostasis of lipids, carbohydrates, and proteins and, therefore, the integrity of the host health. Recent studies have pointed out the existence of an intense cross-talk between the liver (as a metabolically active tissue) and the immune system. The hepatic infiltration of neutrophils and mononuclear cells, as well as the release of large amounts of inflammatory cytokines that participate in the early defense response, plays a role against the parasite's invasion of the liver. Their participation is critical for host defense but can cause additional liver damage. The clearance of extracellular trypomastigotes is optimized by the coordinated cooperation of antibodies and phagocytes, a process that results in efficient parasite destruction when phagocytes are primed by inflammatory cytokines, notably by IFNγ (Plata et al., 1984).

Peroxisome proliferator-activated receptors (PPARs), the nuclear hormone receptor superfamily, are transcription factors that bind DNA and regulate transcription in a ligand-dependent manner. They regulate gene expression after binding Retinoid X Receptor (RXR) as a heterodimeric partner to specific DNA sequence elements termed peroxisome-proliferator response elements (Tugwood et al., 1992). PPARs are ligand-dependent nuclear transcription factors that have emerged as regulators of lipid metabolism and inflammation. The natural ligand 15-deoxy-$\Delta^{12,14}$ prostaglandin J2 (15dPGJ2) has high affinity for PPARγ and is a potent anti-inflammatory molecule. It has been previously described that 15dPGJ2 can repress inflammatory genes, including those coding for nitric oxide synthase 2 (NOS2), cyclooxygenase 2 (COX2) and tumor necrosis factor α (TNF-α), in activated macrophages and cardiomyocytes from *T. cruzi*-infected mice, and that this repression is partially dependent on PPARγ expression (Hovsepian et al., 2011, 2010; Straus et al., 2000). Also, it has been reported that treatment with 15dPGJ2 reduces the inflammatory infiltrate in the skeletal muscle at the site of infection (Rodrigues et al., 2010).

In the liver, PPARs have important functions. Among these, they contribute to maintaining hepatic stellate cells in a quiescent condition, because their activation and transformation are considered the reasons for the origin and development of liver fibrosis upon their transdifferentiation to fibrogenic myofibroblasts; indeed, PPARγ is able to inhibit type I collagen expression at the level of transcription (Miyahara et al., 2000).

In this work, we investigated the role of the treatment with 15dPGJ2, a PPARγ natural ligand, as a modulator of liver inflammation, hepatic function and fibrosis in mice infected with *T. cruzi*.

2. Materials and methods

2.1. In vivo model: mice and infection

Mice used in this study were bred and maintained at the animal facility of the Instituto de Investigaciones en Microbiología y Parasitología Médica, Universidad de Buenos Aires–CONICET. All procedures carried out with mice were approved by the Institutional Committee for the Care and Use of Laboratory Animals (CICUAL, Facultad de Medicina de la Universidad de Buenos Aires, CD 2271/2014) and are in accordance with guidelines of the Argentinean National Administration of Medicines, Food and Medical Technology (ANMAT), Argentinean National Service of Sanity and Agrifoods Quality (SENASA) and also based on the US NIH Guide for the Care and Use of Laboratory Animals. Eight-week-old BALB/c male mice (7 per group) were infected intraperitoneally with 1×10^5 bloodstream trypomastigotes of the lethal RA (pantropic/reticulotropic) strain of *T. cruzi* as previously described (Celentano and González Cappa, 1993). Mice were sacrificed by CO_2 exposure at 6, 24, 36 and 48 h post-infection (p.i.) or at 10 days post-infection (d.p.i.), depending on the experimental protocol. This day was chosen because at this moment the animals didn't show wasting signs, although they had mounted a significant inflammatory response. Daily monitoring of mice health was performed without unexpected deaths. In addition, some RA-infected mice were treated i. p with 15dPGJ2 (1 mg/kg) (Cayman Chemical Co, USA) every 12 h or 24 h (depending on the experimental protocol). Each experiment was carried out three times.

2.2. Parasitemia and survival

Presence of parasites in blood was evaluated by the microhematocrit method (Feilij et al., 1983). Parasitemia was analysed periodically using Pizzi's technique modified by Brener (1962) and survival was observed daily, until the end of the experiment. Parasitemia was expressed as parasites *per* milliliter of blood.

2.3. Histopathological studies

Livers from *T. cruzi*-infected and 15dPGJ2-treated infected mice were fixed in 4% paraformaldehyde in 1× PBS, dehydrated and embedded in paraffin. Six non-contiguous sections (5 μm) were cut and stained with hematoxylin-eosin or Masson Trichrome stain. Cellular infiltrates, presence of amastigote nests and collagen deposition were examined using a Nikon Eclipse E600 microscope (Nikon Inc.). Images were captured with a Spot RT digital camera. At least thirty random microscopic fields (400×) were analysed in each microscopic section, using the open source Image J software (NIH, USA).

2.4. mRNA and gDNA purification

Total RNA was obtained from liver tissue homogenates using Quickzol reagent (Kalium), treated with DNAse (Life Technologies) and total RNA was reversed transcribed using Expand Reverse Transcriptase (Promega Corporation), following the manufacturer's instructions.

gDNA was obtained from liver tissue using phenol-chloroform extraction (Laird et al., 1991).

2.5. Quantitative real-time polymerase chain reaction (qPCR and RT-qPCR)

Both qPCR and RT-qPCR were performed using 5× HOT FIREPOL EVAGREEN qPCR (Solis BioDyne) in an Applied Biosystems 7500

sequence detector. mRNA expression was analysed by RT-qPCR. The parameters were: 52 °C for 2 min, 95 °C for 15 min, and 40 cycles of 95 °C for 15 s, 64 °C (for TCZ), 63 °C (for TGF-β and CTGF), 60 °C (for IL-6, TNF-α, IL-10 and 18S rRNA) or 57 °C (for IL-1β), for 30 s and 72 °C for 1min. Expression of 18S rRNA was analysed in the samples in the same run, for normalization purposes.

The parasite load in the liver was quantified by qPCR using gDNA as template, amplifying the highly repetitive and specific sequence TCZ (Cummings and Tarleton, 2003; Duffy et al., 2009). These primers amplify a 146-bp sequence of the highly repetitive (104 repeats) satellite genomic DNA. The high number of copies increases the sensitivity of the technique allowing the detection of less than 1 parasite/ml, which is defined as parasite equivalents.

Quantification was performed using the comparative threshold cycle (Ct) method and efficiency of the RT reaction (relative quantity, $2^{-\Delta\Delta Ct}$). The replicates were then averaged and fold induction was determined, considering the value at zero time as 1 (Schmittgen and Livak, 2008).

Primer sequences were: *TCZ*: Fw 5′ TCCCTCTCATCAGTTCTATGGCCC 3'; Rv 5′ CAGCAAGCATCTATGZCACTTAGACCCC 3'. *TNF-α*: Fw 5′ GCTCTTGCCCACAMGGGTGC 3'; Rv 5′ CCAAGCAGCGGATAGTTCAG 3'. *IL-6*: Fw 5′ TGATGCACTTGCAGAAAACAA 3'; Rv 5′ GGTCTTGGTCCTTAGCCACTC 3'. *IL-1β*: Fw 5′ TTGACAGTGATGAGAATGACC 3'; Rv 5′ CAAAGATGAAGGAAAAGAAGG 3'. *CTGF*: 5′ Fw CCTAAAATCGCCAAGCCTGT 3'; Rv 5′ CACCCCGCAGAACTTAGCC 3'. *TGF-β*: Fw 5′ CACCGGAGAGCCCTGGATA 3'; Rv 5′ TGTACAGCTGCCGCACACA 3'. *IL-10*: Fw 5′ CTCCCCTGTGAAAATAAGAGCA 3'; Rv 5′ TCCAGCAGACTCAATACACACT 3'. *PPARγ*: Fw 5′ ATCTACACGATGCTGGC 3'; Rv 5′ GGATGTCCTCGATGGG 3'. *18S*: Fw 5′ AACACGGGAAACCTCACCC 3'; Rv 5′ CCACCAACTAAGAACGGCCA 3'.

2.6. Preparation of cytosolic, nuclear and total protein extracts for western blot

Liver tissue (100 mg) was homogenized with 300 μl of Buffer A (10 mmoL/L HEPES pH = 7.90, 1 mmoL/L EDTA, 1 mmoL/L EGTA, 10 mmoL/L KCl, 1 mmoL/L DTT, 0.5 mmoL/L PMSF, 40 mg/L leupeptin, 2 mg/L tosyl-lysyl-chloromethane, 5 mmoL/L NaF, 1 mmoL/L $NaVO_4$, 10 mmoL/L Na_2MoO_4) and NP-40 (Life Technologies) was added to reach 0.5% (v/v). After 15 min at 4 °C, the tubes were gently vortexed for 10 s, and cytosolic extracts were collected by centrifugation at 13000*g* for 90 s. The supernatants were stored at −20 °C (cytosolic extracts), and liver pellets were resuspended in 100 μl buffer A supplemented with 20% (v/v) glycerol and 0.4 M KCl, and mixed for 30 min at 4 °C. Nuclear proteins were obtained by centrifugation at 13000*g* for 5 min, and aliquots of the supernatant (nuclear extracts) were stored at −80 °C.

Total protein extracts were obtained after washing the livers with PBS and adding 300 μl of RIPA modified lysis buffer (150 mM NaCl, 50 mM Tris-HCl (pH = 7.40), 1% Triton X-100, 1 mM EDTA, 1 mM PMSF; 2.5 g/L Protease Inhibitor Cocktail (Sigma Aldrich), 1 mM Na_3VO_4, 1 mM NaF). Then, the tubes were kept on ice for 30 min with swirling and the samples were centrifuged at 7000 g at 4 °C for 10 min. The supernatant was stored at −20 °C. Protein concentrations of sera and protein extracts were determined by the Bradford method using the Bio-Rad Protein Assay (Bio-Rad, USA) reagent and bovine serum albumin (BSA) (Sigma-Aldrich Co.) as a standard (Kruger, 1994).

2.7. Western blot analysis

Proteins extracts were boiled in Laemmli sample buffer and equal amounts of protein (50–100 μg) were separated by 8–12% SDS-PAGE. The gels were blotted onto a Hybond-P membrane (GE Healthcare, Madrid, Spain) and incubated with the following antibodies: anti-NOS2, anti- IκB-α, anti-p65, anti-MMP2 (Santa Cruz Biotechnology, CA, USA), and anti-α-actin (Sigma-Aldrich Co). The blots were revealed by enhanced chemiluminescence (ECL) in an ImageQuant 300 Imager (GE Healthcare Biosciences, USA) following the manufacturer's instructions. Band intensity was analysed using the open source ImageJ software (NIH, USA, http://imagej.nih.gov/ij/).

2.8. Electrophoretic mobility shift assays (EMSA)

The oligonucleotide sequence 5′ TGCTAGGGGGATTTT CCCTCTCTCTGT 3', corresponding to the consensus NF-κB binding site (nucleotides−978 to−952) of the murine NOS2 promoter, was annealed with the complementary sequence by incubation for 5 min at 85 °C in 10 mmol/l Tris–HCl, pH 8.0, 50 mmoL/l NaCl, 10 mmoL/l $MgCl_2$ and 1 mmoL/l dithiothreitol. Aliquots (100 ng) were end-labeled with T4 Polynucleotide Kinase I in the presence of 50 μCi of [α-^{32}P] dCTP and the other unlabeled dNTPs in a final volume of 50 μl. DNA probe (5×10^4 d.p.m.) was used for each binding assay: 5 μg of nuclear liver proteins was incubated for 15 min at 4 °C with the probe and with 1 μg of poly (dI–dC), 5% glycerol, 1 mmoL/l EDTA, 10 mmoL/l KCl, 5 mmol/l $MgCl_2$, 1 mmoL/l dithiothreitol, and 10 mmoL/l Tris–HCl (pH 7.8) in a final volume of 20 μl. The DNA–protein complexes were separated on native 6% polyacrylamide gels in 0.5% Tris–borate–EDTA buffer. Supershift assays were carried out after the addition of the antibody against NF-κB protein (p65) (0.5 μg) to the binding reaction and incubation for 1 h at 4 °C before the addition of the probe. Analysis of competition with unlabeled oligonucleotides was performed using a 20-fold excess of double stranded DNA in the binding reaction and adding the nuclear extracts as the last step in the binding assay. Unrelated competitor oligonucleotide AP-1 (consensus) corresponding to the AP-1 motif of the albumin promoter, 5′ TTCCAAAGAGTCATCAG 3′ was used to ensure band specificity.

2.9. De Ritis Ratio

As a biochemical marker of hepatocellular damage, the De Ritis Ratio (GOT/GPT) was calculated (Botros and Sikaris, 2013). The activity of glutamate oxaloacetate transaminase (GOT/AST) and glutamate pyruvate transaminase (GPT/ALT) were determined, using commercially available assay kits according to the manufacturer's instructions (Wiener Lab, Rosario, Argentina). The kit relies on the reduction of $NADP^+$ and the increase in absorbance measured at 340 nm.

2.10. Statistical analysis

Data are expressed as mean of three independent experiments ± SEM for each treatment (7 mice/group). The Kaplan-Meier test was used to compare survival curves between groups. One-way ANOVA was used to analyze the statistical significance of the differences observed between the infected, treated or untreated groups. The Tukey post-hoc test was performed to compare all pairs of groups. Student's *t*-test was used to analyze statistical significance of the differences in the number of inflammatory infiltrates and amastigote nests between infected and infected 15dPGJ2-treated mice and Kruskall-Wallis test and Dunns post-hoc test was used to analyze differences in collagen deposition between uninfected, *T. cruzi*-infected and *T. cruzi*-infected 15dPGJ2-treated mice. Differences were considered statistically significant when $P < 0.05$. All analyses were performed using the Prism 5.01 Software (GraphPad, USA).

3. Results

3.1. 15dPGJ2 and course of infection

To assess the role of 15dPGJ2 in preventing liver inflammation and fibrosis, BALB/c mice were infected with 1×10^5 trypomastigotes of the lethal *T. cruzi* strain RA via the intraperitoneal route. Initially, we determined PPARγ mRNA expression in the liver of infected mice to asses the role of PPARγ in the effects of 15dPGJ2. We found a significant increase in PPARγ mRNA levels in the livers of infected mice in comparison with uninfected ones. Moreover, no significant differences were observed in the PPARγ mRNA levels of *T. cruzi*-infected, and *T. cruzi*-infected and 15dPGJ2-treated mice (Fig. 1A). Similar parasitemia levels were found in *T. cruzi*-infected and *T. cruzi*-infected and 15dPGJ2-treated mice between 3 and 8 d.p.i., with a trend to higher parasitemia in 15dPGJ2-treated mice at day 10 p.i. (Fig. 1B). The parasite load in the liver at the moment of euthanasia (10 d.p.i.), was quantified with gDNA by qPCR using TCZ primers. No significant differences were observed between both groups (Fig. 1C). The body weight of infected mice treated with 15dPGJ2 remained unchanged throughout the study (Fig. 1D). Consistent with parasitemia levels and in agreement with results previously reported by our group Penas et al. (2013), survival of mice in both *T. cruzi*-infected and *T. cruzi*-infected and 15dPGJ2-treated groups was similar. These mice did not survive longer than 15 d.p.i. (Kaplan-Meyer test, data not shown).

3.2. Inflammatory reaction is reduced by 15dPGJ2 in the liver of *T. cruzi*-infected mice

It has been described that PPARγ ligands participate in the control of the inflammatory response. One of the first aims of this work was to analyze the effects of 15dPGJ2 on the livers of *T. cruzi*-infected mice. Therefore, mice were treated with 15dPGJ2 (1 mg/kg) every 24 h, from the first day after infection until the day before sacrifice.

Mice infected with *T. cruzi* showed intense inflammatory reaction, consisting of mononuclear cell infiltrates. Treatment with 15dPGJ2 significantly reduced liver inflammation (number of inflammatory foci/field, *T. cruzi* vs. *T. cruzi*+15dPGJ2, 0.62 ± 0.21 vs. 0.18 ± 0.02, $p < 0.05$, Fig. 2A). No differences in the number of amastigote nests *per* field were observed between the infected and infected and treated groups (Fig. 2A).

To evaluate the expression of pro-inflammatory cytokines, mice were treated with 15dPGJ2 (1 mg/kg) every 12 h. They were evaluated at 24 h post infection considering that, in previous studies, we observed a peak for these cytokines in cardiac tissue at that time, decaying thereafter (Penas et al., 2013). Fig. 2B shows that the liver tissue of infected mice expressed considerable amounts of TNF-α, IL-6 and IL-1β mRNA, measured by RT-qPCR, with a significant peak at 24 h p.i. and decreasing at 36 h p.i. These inflammatory cytokines were significantly inhibited in the livers of 15dPGJ2-treated mice (Fig. 2B). Based on the fact that 15dPGJ2 treatment inhibited inflammatory cytokines, we also evaluated the expression of pro-inflammatory enzymes in livers of *T. cruzi*-infected and treated mice. As shown in Fig. 2C, livers from *T. cruzi*-infected mice expressed NOS2 and MMP2 at 10 d.p.i. and 15dPGJ2 treatment inhibited both NOS2 and MMP2 protein expression.

3.3. 15dPGJ2 attenuates liver fibrosis, liver injury biomarkers and pro-fibrotic cytokines

Fibrosis was observed in liver sections of *T. cruzi*-infected mice, as shown by Masson trichrome stain. Collagen deposits were found in interstitial tissue and perisinusoidal areas. Treatment of infected mice with 15dPGJ2 significantly reduced fibrosis (*T. cruzi* vs. *T. cruzi* +15dPGJ2, Kruskal-Wallis, $p < 0.0001$, Dunns post-test:

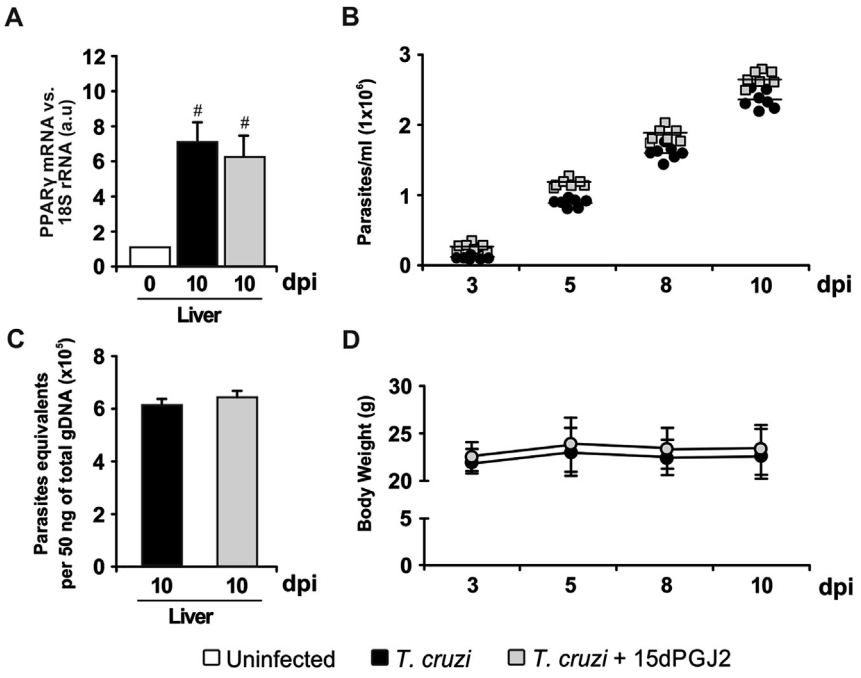

Fig. 1. Effect of 15dPGJ2 on the course of infection. BALB/c mice were infected with 1×10^5 trypomastigotes of the lethal RA *T. cruzi* strain by intraperitoneal route and treated daily with 1 mg/kg/day 15dPGJ2. (A) Expression of PPARγ mRNA was measured in the liver of *T. cruzi*-infected and *T. cruzi*-infected and 15dPGJ2-treated mice by RT-qPCR. The results were normalized against 18S rRNA. (B) Parasitemia was analysed until day 10 p.i. (C) Parasite load was detected by qPCR in the liver of *T. cruzi*-infected and *T. cruzi*-infected and 15dPGJ2-treated mice, using gDNA as template. (D) Body weight was registered in the experimental groups during the course of infection. Results shown are the mean and SD of a representative experiment out of 3 performed. #, $P < 0.05$ vs. uninfected.

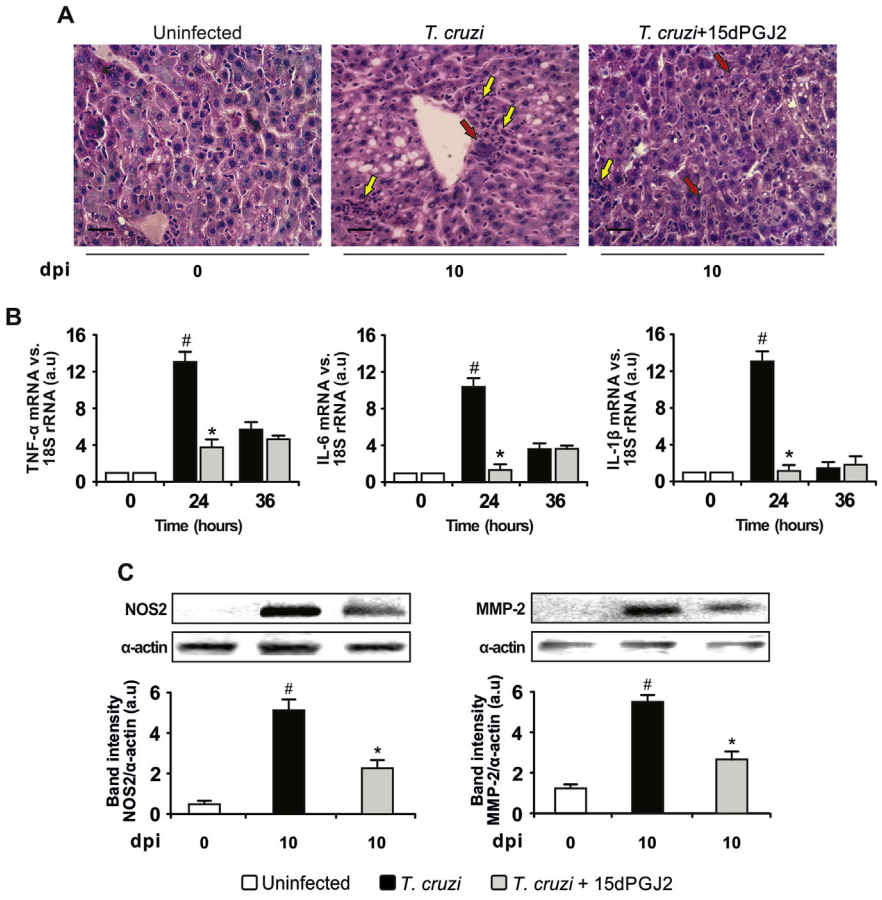

Fig. 2. 15dPGJ2 reduces liver inflammatory reaction in *T. cruzi*-infected mice. (A) Liver inflammatory reaction and parasite nests were analysed at 10 d.p.i. in histological sections of *T. cruzi*-infected, *T. cruzi*-infected and 15dPGJ2-treated and uninfected mice, stained with hematoxilin-eosin (bar: 100 μm, yellow arrows, inflammatory infiltrates, red arrows, amastigote nests). (B) Pro-inflammatory cytokines (TNF-α, IL-6 and IL-1β), were analysed by RT-qPCR. The results were normalized against 18S rRNA. (C) NOS2 and MMP-2 expression were analysed by Western-blot from livers of the different experimental groups. Protein levels were normalized against α-actin. Results represent the mean ± SEM of three independent experiments. *, $P < 0.05$ vs. *T. cruzi*. #, $P < 0.05$ vs. uninfected. (For interpretation of the references to colour in this figure legend, the reader is referred to the web version of this article.)

T. cruzi vs. *T. cruzi*+15dPGJ2, p < 0.0001, Uninfected vs. *T. cruzi*+15dPGJ2, ns) (Fig. 3A).

In addition, we evaluated the GOT and GPT serum activities as typical biochemical markers of liver function, after *T. cruzi* infection and 15dPGJ2 treatment. Our results showed a significant increase in the De Ritis ratio (GOT/GPT) after infection in comparison with uninfected mice. Remarkably, this ratio dropped to normal values when mice were treated with 15dPGJ2 (Fig. 3B). The same phenomenon was observed when we analysed markers of pro-fibrotic activity, like connective tissue growth factor (CTGF) and TGF-β. Higher levels of expression of CTGF and TGF-β were detected by RT-qPCR in liver extracts from infected mice in comparison with uninfected animals. Moreover, treatment with 15dPGJ2 significantly inhibited CTGF (Fig. 3C) and TGF-β expressions (Fig. 3D). Besides, we determined the mRNA expression of IL-10, a characteristic anti-inflammatory cytokine, in livers of infected and treated mice. We verified that 15dPGJ2 significantly increased the expression of IL-10 in livers from infected and treated mice (Fig. 3E).

3.4. 15dPGJ2 inhibits NF-κB activation in livers of infected mice

In this work, we determined the activation of NF-κB and the role of 15dPGJ2 in the livers of infected and treated mice. To this aim we determined the cytosolic expression and disappearance of IκB-α and NF-κB p65 subunit, in the livers of *T. cruzi*-infected mice. Fig. 4A shows that NF-κB was activated, since IκB-α and p65 begin to disappear in the cytosolic extracts at 24 h p.i. and this effect continues, at least, up to 48 h p.i. Furthermore, EMSA confirmed the translocation of p65– NF-κB subunit to the nucleus 48 h after infection in nuclear extracts of liver tissue (Fig. 4C).

In view of the activation of NF-κB, we next asked whether the effects of 15dPGJ2 or PPARγ were exerted through the NF-κB pathway. Infected mice were treated with 15dPGJ2 and liver protein extracts were analysed by Western blot. Fig. 4B shows that treatment with 15dPGJ2 precludes p65–NF-κB translocation to the nucleus. Moreover, EMSA also confirmed that treatment with 15dPGJ2 inhibits NF-κB activation, at 48 h in *T. cruzi*-infected mice (Fig. 4C).

4. Discussion

In this study, we focused on the ability of 15dPGJ2 to regulate the serum activity of typical biochemical markers of hepatic function, pro-fibrotic cytokines and pro-inflammatory mediators in the liver of *T. cruzi*-infected mice. An acute model of infection with the lethal *T. cruzi* strain RA (DTU VI) was used.

Our results demonstrate that 15dPGJ2 treatment did not modify the parasite load in hepatic tissue. The trend to higher parasitemia associated with 15dPGJ2 treatment in *T. cruzi* infected mice was not substantial from a biological point of view. Same interpretation can

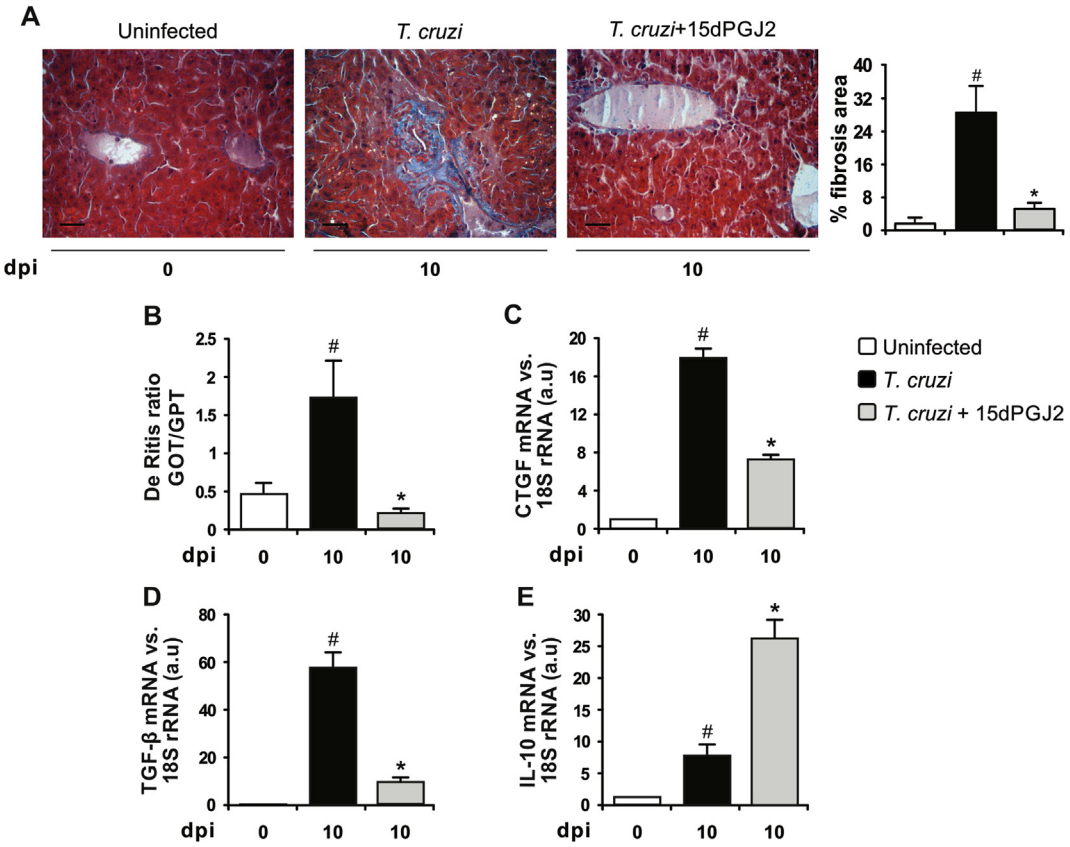

Fig. 3. 15dPGJ2 reduces liver fibrosis in *T. cruzi*-infected mice. (A) Collagen deposits in liver sections of *T. cruzi*-infected, *T. cruzi*-infected and 15dPGJ2-treated and uninfected mice, stained with Masson trichrome (bar: 100 μm). Bar graph shows the % fibrosis area (Mean ± SEM of three independent experiments). (B) The De Ritis ratio (GOT/GPT) was assessed in liver homogenates of the different experimental groups. (C) CTGF, (D) TGF-β and (E) IL-10 mRNA expression was analysed by RT-qPCR in liver homogenates of the different experimental groups. All studies were performed at 10 d.p.i. For C, D and E results were normalized against 18S rRNA. Results represent the mean ± SEM of three independent experiments. *, $P < 0.05$ vs. *T. cruzi*. #, $P < 0.05$ vs. uninfected.

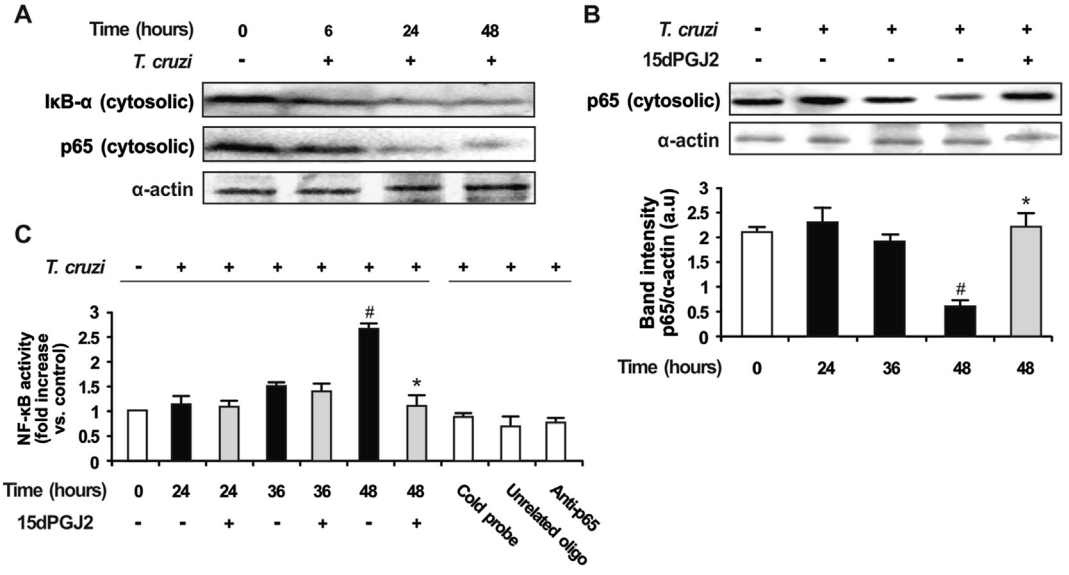

Fig. 4. 15dPGJ2 inhibits NF-κB pathway in the liver of *T. cruzi*-infected mice. (A) and (B) Expression of IκB-α and NF-κB p65 subunit was determined by Western-blot with specific antibodies in liver homogenates of uninfected, *T. cruzi*-infected and *T. cruzi*-infected and 15dPGJ2-treated mice. (C) Electrophoretic mobility shift assays (EMSA) were carried out for determination of NF-κB activation in the livers of uninfected, *T. cruzi*-infected and *T. cruzi*-infected and 15dPGJ2-treated mice. Competition assays with excess of unlabeled oligonucleotide and an unrelated competitor oligonucleotide (AP-1) were used to ensure band specificity. Supershift assays was performed after incubation of the nuclear extracts with anti-p65, and the corresponding p50/p65 complex was identified. The protein-DNA complexes representing heterodimer p50/p65 was quantified by Image J. Results represent the mean ± SEM of three independent experiments. *, $P < 0.05$ vs. *T. cruzi* 48 h #, $P < 0.05$ vs. uninfected.

be given to the increase in parasitemia previously reported by our group since, while it was statistically significant, the order of magnitude of the parasitemia was the same in both groups (Penas et al., 2013). While the trend to increased parasitemia may reflect NOS2 inhibition and the consequent diminished NO levels, Marinho et al. (2007) using a non-lethal *T. cruzi* strain showed that NOS2−KO mice are able to control parasitemia and tissue parasitism. The explanation for these controversial results may lay in the genetic differences in the strains of *T. cruzi* and mouse used.

Moreover, body weight of infected and treated mice remained unchanged all over the study. On the contrary, 15dPGJ2 was able to inhibit the increase of the De Ritis ratio (a marker of liver dysfunction), liver inflammatory reaction and fibrosis. This inhibition was due, at least in part to PPARγ-independent mechanisms, since NF-κB was inactivated by the treatment.

Previously, we reported that 15dPGJ2 modulates the inflammatory response in the heart from mice infected with *T. cruzi* strains of different lethality (Penas et al., 2013). However, its effect on liver inflammation during *T. cruzi* infection had not been addressed before. Results presented here demonstrate, for the first time, that treatment with 15dPGJ2 reduced liver inflammation, since mononuclear cell infiltrates were significantly inhibited. Similarly, pro-inflammatory cytokines like TNF-α, IL-1β and IL-6, substantially expressed after infection, were also inhibited in the liver after the treatment. Recently, an important role for TNF-α in the liver of C57BL/6 mice infected with *T. cruzi* has been suggested, since anti-TNF-α antibodies inhibit the induction of tissue injury (Ronco et al., 2010). Besides, our data showed that 15dPGJ2 inhibits the expression and activity of pro-inflammatory enzymes such as NOS2 and MMP2 in the liver, which may be considered as a mechanism to control overt inflammatory reaction leading to tissue damage. NO is produced by different isoforms of NOS, including NOS2, which increases in the liver of infected mice matching the increase of TNF-α, IL-1β and IL-6, as shown by our results. Moreover, the inhibitory effects of 15dPGJ2 would not be potentiated through the early induction of an anti-inflammatory cytokine like IL-10, since mRNA levels for this cytokine remained unchanged at 24 h in *T. cruzi*-infected 15dPGJ2-treated mice (data not shown). While the proinflammatory response contributes to an effective parasite clearance, its excessive expression may be deleterious for the host. In this regard, it has been described that NOS2 is expressed in hepatic cells in pathological conditions and that its induction is involved in the development of liver fibrosis (Iwakiri, 2015). The role of NOS2 in liver fibrosis has been studied using NOS2-knockout mice or NOS2 inhibitors *in vivo* and *in vitro*. The results showed that, under these conditions, liver fibrosis is reduced, suggesting that NOS2 could be a therapeutic target for liver fibrosis (Anavi et al., 2015; Aram et al., 2008).

Other factors, including parasite persistence in the heart tissue, contribute to Chagas disease and damage of different tissues (Marin-Neto et al., 2007). In this sense, it has been described that the MMP family may also contribute to the development of chagasic cardiomyopathy, facilitating parasitic infection and persistence. In this regard, treatment with an MMP inhibitor significantly decreases heart inflammation (Gutierrez et al., 2008).

It has been described that viral infection, autoimmune diseases, obesity/metabolic syndrome, alcohol abuse, and non-alcoholic hepatic steatohepatitis may act as primary drivers of chronic liver injury which could lead to fibrosis (Bataller and Gao, 2015; Iwakiri, 2015; Peng et al., 2009; Schuppan and Kim, 2013). Progression of liver fibrosis eventually leads to cirrhosis, which can be associated with hepatocellular carcinoma and liver failure (Coulouarn and Clément, 2014). Moreover, it has been recently demonstrated that *T. cruzi* infection must be considered as an additional risk factor because it exacerbates the inflammation and accelerates the development of hepatic injury (Onofrio et al., 2015). In this study, we showed that treatment of *T. cruzi*-infected mice with 15dPGJ2 significantly reduced liver fibrosis and restored the De Ritis ratio to normal values, suggesting that it prevents liver damage. Consistently with these results, 15dPGJ2 treatment also inhibited markers of pro-fibrotic activity like TGF-β and CTGF, as evaluated by RT-qPCR.

It has been suggested that myofibroblasts, the key factor of fibrogenesis, are highly proliferative cells that exhibit enhanced survival. These cells migrate to and accumulate at sites of liver injury in response to various growth factors, cytokines, lipid mediators, or adipokines, produced by the injured liver (Mallat and Lotersztajn, 2013). Current knowledge confers a crucial role to CTGF in hepatic fibrogenesis. Hepatocytes are likely to be the main cellular source of CTGF in the liver, which is upregulated by TGF-β. In 2009, Gressner et al. (2009) performed a clinical study in which they determined that caffeine leads to upregulation of PPARγ expression in hepatocytes, thus sensitizing these cells to the well-known inhibitory effect of 15dPGJ2 on CTGF expression. Earlier reports showed that 15dPGJ2 has a potent inhibitory effect on TGF-β-induced CTGF expression in the liver upon receptor binding (Gressner et al., 2008; Sun et al., 2006; Zhao et al., 2006). While receptor expression seems to be a limiting factor, our results show that 15dPGJ2 treatment increases PPARγ expression in the livers from *T. cruzi*-infected mice, which favors the inhibitory ligand action. We also showed herein that 15dPGJ2 treatment increases IL-10 levels in the livers of infected mice, thus playing a compensatory role in front of the expression of proinflammatory cytokines. Carrera-Silva et al. (2010) showed that liver leukocytes from infected B6 mice produce increased and persistent levels of pro-inflammatory cytokines, associated with undetectable or low IL-10 and TGF-β production. Also, it has been shown that IL-10 knockout mice are more susceptible to infection and have higher mortality rates than wild-type mice (Hunter et al., 1997; Roffê et al., 2012). In this regard, we have previously reported that treatment with exogenous IL-10 inhibits the production of pro-inflammatory mediators through up-regulation of SOCS-3 in *T. cruzi*-infected cardiomyocytes (Hovsepian et al., 2013). Furthermore, it has been reported that peripheral blood mononuclear cells isolated from patients in the indeterminate phase of Chagas' disease produce higher levels of IL-10 than those isolated from patients with chronic cardiomyopathy (Gomes et al., 2003; Souza et al., 2004). Thus, 15dPGJ2 might be exerting its anti-inflammatory role in the liver through induction of IL-10. This increase might also be due to the activation of non-canonical NF-κB involving the formation p50 homodimers (Cao et al., 2006).

Herein, we demonstrated that NF-κB is activated in the liver after *T. cruzi* infection and that this pathway is inhibited by 15dPGJ2 treatment. It has been demonstrated that 15dPGJ2 actions are exerted by means of a PPARγ-independent mechanism, involving intracellular targets in the NF-κB signaling pathway (Hovsepian et al., 2011; Penas et al., 2013; Rossi et al., 2000; Straus et al., 2000). Here we showed that 15dPGJ2 treatment modulates NF-κB activation, preventing p65 nuclear translocation in the livers from *T. cruzi*-infected mice, as shown by EMSA, reinforcing the idea of the broad target tissue effects of 15dPGJ2 on the elicitation of PPAR-dependent and -independent anti-inflammatory mechanisms. Because NF-κB has a pivotal role in the regulation of inflammation and cell survival (Papa et al., 2009) a fine tuned targeting to this factor may be needed to properly treat diseases in which its dysregulation is involved. It must be noted, however, that in our model NF-κB plays a clear role in the promotion of the inflammatory response and, most important, treatment with 15dPGJ2, which precludes its activation, results in a beneficial outcome in terms of tissue inflammation and functional restoration.

Our results demonstrate that 15dPGJ2 elicits potent anti-inflammatory effects in the liver of *T. cruzi*-infected mice. This is evidenced by the restoration of the De Ritis ratio to normal values, the inhibition of pro-fibrotic cytokines induced by infection and the reduction of inflammatory mediators in the liver function during the course of acute *T. cruzi* infection.

Most of the deleterious effects associated with *T. cruzi* infection are related to the persistent inflammatory response leading to tissue fibrosis and organ dysfunction. Therefore, prevention of inflammation and its progression to fibrosis in a broad range of tissues, through the use of PPARγ agonists as coadjuvants of anti-parasitic treatment, may contribute to a better outcome of the disease.

Funding

This work was supported by Consejo Nacional de Investigaciones Científicas y Técnicas (CONICET, grant PIP 0672) to N. B. Goren, Universidad de Buenos Aires (grant UBACyT 20020130100774BA) to N. B. Goren, Fundación "Alberto J. Roemmers" to F. Penas and Fundación "Bunge y Born" to F. Penas, Argentina.

Conflict of interest

The authors have no conflict of interest.

Acknowledgements

We are grateful to Mr. Eduardo Alejandro Giménez and Mr. Ricardo Chung for their excellent technical assistance. We would also like to thank Ms. Victoria González Eusevi for her assistance in English grammar and spelling corrections.

References

Anavi, S., Eisenberg-Bord, M., Hahn-Obercyger, M., Genin, O., Pines, M., Tirosh, O., 2015. The role of iNOS in cholesterol-induced liver fibrosis. Laboratory investigation; A J. Tech. Methods Pathol. 95, 914–924.

Aram, G., Potter, J.J., Liu, X., Torbenson, M.S., Mezey, E., 2008. Lack of inducible nitric oxide synthase leads to increased hepatic apoptosis and decreased fibrosis in mice after chronic carbon tetrachloride administration. Hepatol. Baltim. Md. 47, 2051–2058.

Barreto-de-Albuquerque, J., Silva-dos-Santos, D., Pérez, A.R., Berbert, L.R., de Santana-van-Vliet, E., Farias-de-Oliveira, D.A., Moreira, O.C., Roggero, E., de Carvalho-Pinto, C.E., Jurberg, J., Cotta-de-Almeida, V., Bottasso, O., Savino, W., de Meis, J., 2015. *Trypanosoma cruzi* infection through the oral route promotes a severe infection in mice: new disease form from an old infection? PLoS Neglected Trop. Dis. 9, e0003849.

Bataller, R., Gao, B., 2015. Liver fibrosis in alcoholic liver disease. Seminars liver Dis. 35, 146–156.

Botros, M., Sikaris, K.A., 2013. The de ritis ratio: the test of time. The Clinical biochemist. Rev./Aust. Assoc. Clin. Biochem. 34, 117–130.

Brener, Z., 1962. Observations on immunity to superinfections in mice experimentally inoculated with *Trypanosoma cruzi* and subjected to treatment. Rev. do Inst. Med. Trop. Sao Paulo 4, 119–123.

Cao, S., Zhang, X., Edwards, J.P., Mosser, D.M., 2006. NF-kappaB1 (p50) homodimers differentially regulate pro- and anti-inflammatory cytokines in macrophages. J. Biol. Chem. 281, 26041–26050.

Carrera-Silva, E.A., Guiñazu, N., Pellegrini, A., Cano, R.C., Arocena, A., Aoki, M.P., Gea, S., 2010. Importance of TLR2 on hepatic immune and non-immune cells to attenuate the strong inflammatory liver response during *Trypanosoma cruzi* acute infection. PLoS Neglected Trop. Dis. 4, e863.

Celentano, A.M., González Cappa, S.M., 1993. *In vivo* macrophage function in experimental infection with *Trypanosoma cruzi* subpopulations. Acta Trop. 55, 171–180.

Coulouarn, C., Clément, B., 2014. Stellate cells and the development of liver cancer: therapeutic potential of targeting the stroma. J. Hepatol. 60, 1306–1309.

Cummings, K.L., Tarleton, R.L., 2003. Rapid quantitation of *Trypanosoma cruzi* in host tissue by real-time PCR. Mol. Biochem. Parasitol. 129, 53–59.

Duffy, T., Bisio, M., Altcheh, J., Burgos, J.M., Diez, M., Levin, M.J., Favaloro, R.R., Freilij, H., Schijman, A.G., 2009. Accurate real-time PCR strategy for monitoring bloodstream parasitic loads in chagas disease patients. PLoS Neglected Trop. Dis. 3, e419.

Feilij, H., Muller, L., Gonzalez Cappa, S.M., 1983. Direct micromethod for diagnosis of acute and congenital Chagas' disease. J. Clin. Microbiol. 18, 327–330.

Gomes, J.A.S., Bahia-Oliveira, L.M.G., Rocha, M.O.C., Martins-Filho, O.A., Gazzinelli, G., Correa-Oliveira, R., 2003. Evidence that development of severe cardiomyopathy in human Chagas' disease is due to a Th1-specific immune response. Infect. Immun. 71, 1185–1193.

Gressner, O.A., Gao, C., Rehbein, K., Lahme, B., Siluschek, M., Berg, T., Müller, T., Gressner, A.M., 2009. Elevated concentrations of 15-deoxy-Delta12,14-prostaglandin J2 in chronic liver disease propose therapeutic trials with peroxisome proliferator activated receptor gamma-inducing drugs. Liver Int. Official J. Int. Assoc. Study Liver 29, 730–735.

Gressner, O.A., Lahme, B., Rehbein, K., Siluschek, M., Weiskirchen, R., Gressner, A.M., 2008. Pharmacological application of caffeine inhibits TGF-beta-stimulated connective tissue growth factor expression in hepatocytes via PPARgamma and SMAD2/3-dependent pathways. J. Hepatol. 49, 758–767.

Gutierrez, F.R.S., Lalu, M.M., Mariano, F.S., Milanezi, C.M., Cena, J., Gerlach, R.F., Santos, J.E.T., Torres-Dueñas, D., Cunha, F.Q., Schulz, R., Silva, J.S., 2008. Increased activities of cardiac matrix metalloproteinases matrix metalloproteinase (MMP)-2 and MMP-9 are associated with mortality during the acute phase of experimental *Trypanosoma cruzi* infection. J. Infect. Dis. 197, 1468–1476.

Hovsepian, E., Mirkin, G.A., Penas, F., Manzano, A., Bartrons, R., Goren, N.B., 2011. Modulation of inflammatory response and parasitism by 15-Deoxy-Δ(12,14) prostaglandin J(2) in *Trypanosoma cruzi*-infected cardiomyocytes. Int. J. Parasitol. 41, 553–562.

Hovsepian, E., Penas, F., Goren, N.B., 2010. 15-deoxy-Delta12,14 prostaglandin GJ2 but not rosiglitazone regulates metalloproteinase 9, NOS-2, and cyclooxygenase 2 expression and functions by peroxisome proliferator-activated receptor gamma-dependent and -independent mechanisms in cardiac cells. Shock Augusta, Ga. 34, 60–67.

Hovsepian, E., Penas, F., Siffo, S., Mirkin, G.A., Goren, N.B., 2013. IL-10 inhibits the NF-κB and ERK/MAPK-mediated production of pro-inflammatory mediators by up-regulation of SOCS-3 in *Trypanosoma cruzi*-infected cardiomyocytes. PloS One 8, e79445.

Hunter, C.A., Ellis-Neyes, L.A., Slifer, T., Kanaly, S., Grünig, G., Fort, M., Rennick, D., Araujo, F.G., 1997. IL-10 is required to prevent immune hyperactivity during infection with *Trypanosoma cruzi*. J. Immunol. Baltim. Md. 1950 (158), 3311–3316.

Iwakiri, Y., 2015. Nitric oxide in liver fibrosis: the role of inducible nitric oxide synthase. Clin. Mol. Hepatol. 21, 319–325.

Kruger, N.J., 1994. The Bradford method for protein quantitation. Methods Mol. Biol. Clifton, N.J. 32, 9–15.

Laird, P.W., Zijderveld, A., Linders, K., Rudnicki, M.A., Jaenisch, R., Berns, A., 1991. Simplified mammalian DNA isolation procedure. Nucleic Acids Res. 19, 4293.

Mallat, A., Lotersztajn, S., 2013. Cellular mechanisms of tissue fibrosis. 5. Novel insights into liver fibrosis. Am. J. Physiol. Cell Physiol. 305, C789–C799.

Marinho, C.R.F., Nuñez-Apaza, L.N., Martins-Santos, R., Bastos, K.R.B., Bombeiro, A.L., Bucci, D.Z., Sardinha, L.R., Lima, M.R.D., Alvarez, J.M., 2007. IFN-gamma, but not nitric oxide or specific IgG, is essential for the *in vivo* control of low-virulence Sylvio X10/4 *Trypanosoma cruzi* parasites. Scand. J. Immunol. 66, 297–308.

Marin-Neto, J.A., Cunha-Neto, E., Maciel, B.C., Simões, M.V., 2007. Pathogenesis of chronic Chagas heart disease. Circulation 115, 1109–1123.

Miao, Q., Ndao, M., 2014. *Trypanosoma cruzi* infection and host lipid metabolism. Mediat. Inflamm. 2014, 902038.

Miyahara, T., Schrum, L., Rippe, R., Xiong, S., Yee, H.F., Motomura, K., Anania, F.A., Willson, T.M., Tsukamoto, H., 2000. Peroxisome proliferator-activated receptors and hepatic stellate cell activation. J. Biol. Chem. 275, 35715–35722.

Onofrio, L.I., Arocena, A.R., Paroli, A.F., Cabalén, M.E., Andrada, M.C., Cano, R.C., Gea, S., 2015. *Trypanosoma cruzi* infection is a potent risk factor for non-alcoholic steatohepatitis enhancing local and systemic inflammation associated with strong oxidative stress and metabolic disorders. PLoS Neglected Trop. Dis. 9, e0003464.

Papa, S., Bubici, C., Zazzeroni, F., Franzoso, G., 2009. Mechanisms of liver disease: cross-talk between the NF-kappaB and JNK pathways. Biol. Chem. 390, 965–976.

Penas, F., Mirkin, G.A., Hovsepian, E., Cevey, A., Caccuri, R., Sales, M.E., Goren, N.B., 2013. PPARγ ligand treatment inhibits cardiac inflammatory mediators induced by infection with different lethality strains of *Trypanosoma cruzi*. Biochimica Biophysica Acta 1832, 239–248.

Peng, Z., Borea, P.A., Varani, K., Wilder, T., Yee, H., Chiriboga, L., Blackburn, M.R., Azzena, G., Resta, G., Cronstein, B.N., 2009. Adenosine signaling contributes to ethanol-induced fatty liver in mice. J. Clin. Investigation 119, 582–594.

Plata, F., Wietzerbin, J., Pons, F.G., Falcoff, E., Eisen, H., 1984. Synergistic protection by specific antibodies and interferon against infection by *Trypanosoma cruzi* in vitro. Eur. J. Immunol. 14, 930–935. http://dx.doi.org/10.1002/eji.1830141013.

Rodrigues, W.F., Miguel, C.B., Chica, J.E.L., Napimoga, M.H., 2010. 15d-PGJ(2) modulates acute immune responses to *Trypanosoma cruzi* infection. Memorias do Inst. Oswaldo Cruz 105, 137–143.

Roffê, E., Rothfuchs, A.G., Santiago, H.C., Marino, A.P.M.P., Ribeiro-Gomes, F.L., Eckhaus, M., Antonelli, L.R.V., Murphy, P.M., 2012. IL-10 limits parasite burden and protects against fatal myocarditis in a mouse model of *Trypanosoma cruzi* infection. J. Immunol. Baltim. Md. 1950 (188), 649–660.

Ronco, M.T., Francés, D.E., Ingaramo, P.I., Quiroga, A.D., Alvarez, M.L., Pisani, G.B., Revelli, S.S., Carnovale, C.E., 2010. Tumor necrosis factor alpha induced by *Trypanosoma cruzi* infection mediates inflammation and cell death in the liver

of infected mice. Cytokine 49, 64–72.
Rossi, A., Kapahi, P., Natoli, G., Takahashi, T., Chen, Y., Karin, M., Santoro, M.G., 2000. Anti-inflammatory cyclopentenone prostaglandins are direct inhibitors of IkappaB kinase. Nature 403, 103–108. http://dx.doi.org/10.1038/47520.
Sardinha, L.R., Mosca, T., Elias, R.M., do Nascimento, R.S., Gonçalves, L.A., Bucci, D.Z., Marinho, C.R.F., Penha-Gonçalves, C., Lima, M.R.D., Alvarez, J.M., 2010. The liver plays a major role in clearance and destruction of blood trypomastigotes in *Trypanosoma cruzi* chronically infected mice. PLoS Neglected Trop. Dis. 4, e578.
Schmittgen, T.D., Livak, K.J., 2008. Analyzing real-time PCR data by the comparative C(T) method. Nat. Protoc. 3, 1101–1108.
Schuppan, D., Kim, Y.O., 2013. Evolving therapies for liver fibrosis. J. Clin. Investigation 123, 1887–1901.
Souza, P.E.A., Rocha, M.O.C., Rocha-Vieira, E., Menezes, C.A.S., Chaves, A.C.L., Gollob, K.J., Dutra, W.O., 2004. Monocytes from patients with indeterminate and cardiac forms of Chagas' disease display distinct phenotypic and functional characteristics associated with morbidity. Infect. Immun. 72, 5283–5291.
Straus, D.S., Pascual, G., Li, M., Welch, J.S., Ricote, M., Hsiang, C.H., Sengchanthalangsy, L.L., Ghosh, G., Glass, C.K., 2000. 15-deoxy-delta 12,14-prostaglandin J2 inhibits multiple steps in the NF-kappa B signaling pathway. Proc. Natl. Acad. Sci. U. S. A. 97, 4844–4849.
Sun, K., Wang, Q., Huang, X.-H., 2006. PPAR gamma inhibits growth of rat hepatic stellate cells and TGF beta-induced connective tissue growth factor expression. Acta Pharmacol. Sin. 27, 715–723.
Tugwood, J.D., Issemann, I., Anderson, R.G., Bundell, K.R., McPheat, W.L., Green, S., 1992. The mouse peroxisome proliferator activated receptor recognizes a response element in the 5' flanking sequence of the rat acyl CoA oxidase gene. EMBO J. 11, 433–439.
WHO World Health Organization, 2016. WHO Chagas Disease (American Trypanosomiasis).
Zhao, C., Chen, W., Yang, L., Chen, L., Stimpson, S.A., Diehl, A.M., 2006. PPARgamma agonists prevent TGFbeta1/Smad3-signaling in human hepatic stellate cells. Biochem. biophysical Res. Commun. 350, 385–391.